AFRL-SN-RS-TR-2004-44
Final Technical Report
February 2004

STUDY OF LINEARIZATION OF OPTICAL POLYMER MODULATORS

University of Minnesota

APPROVED FOR PUBLIC RELEASE; DISTRIBUTION UNLIMITED.

AIR FORCE RESEARCH LABORATORY
SENSORS DIRECTORATE
ROME RESEARCH SITE
ROME, NEW YORK

STINFO FINAL REPORT

This report has been reviewed by the Air Force Research Laboratory, Information Directorate, Public Affairs Office (IFOIPA) and is releasable to the National Technical Information Service (NTIS). At NTIS it will be releasable to the general public, including foreign nations.

AFRL-SN-RS-TR-2004-44 has been reviewed and is approved for publication.

APPROVED: /s/
BRIAN F. MCKEON
Project Engineer

FOR THE DIRECTOR: /s/
RICHARD G. SHAUGHNESSY, Lt Col, USAF
Chief, Rome Operations Office
Sensors Directorate

REPORT DOCUMENTATION PAGE

Form Approved
OMB No. 074-0188

1. AGENCY USE ONLY (Leave blank)	2. REPORT DATE	3. REPORT TYPE AND DATES COVERED
	FEBRUARY 2004	**FINAL** **Dec 02 – Sep 03**

4. TITLE AND SUBTITLE

STUDY OF LINEARIZATION OF OPTICAL POLYMER MODULATORS

5. FUNDING NUMBERS

G - F30602-03-1-0013
PE - 63175C
PR - 6015
TA - SN
WU - 01

6. AUTHOR(S)

Anand Gopinath, Ross Schermer, Jaesang Oh, Desalegn Bereka

7. PERFORMING ORGANIZATION NAME(S) AND ADDRESS(ES)

University of Minnesota
University of Minnesota Sponsored Projects
200 Oak Street SE
Minneapolis MN 55455-2070

8. PERFORMING ORGANIZATION REPORT NUMBER

N/A

9. SPONSORING / MONITORING AGENCY NAME(S) AND ADDRESS(ES)

AFRL/SNDP
26 Electronic Parkway
Rome NY 13441-4514

10. SPONSORING / MONITORING AGENCY REPORT NUMBER

AFRL-SN-RS-TR-2004-44

11. SUPPLEMENTARY NOTES

AFRL Project Engineer: Brian F. McKeon/SNDP/(315) 330-7348 Brian.McKeon@rl.af.mil

12a. DISTRIBUTION / AVAILABILITY STATEMENT

APPROVED FOR PUBLIC RELEASE; DISTRIBUTION UNLIMITED.

12b. DISTRIBUTION CODE

13. ABSTRACT ***(Maximum 200 Words)***

To improve the Spur Free Dynamic Range of analog electro-optic modulators in the >10 GHz regime, techniques for improving the linearity of these devices must be developed. This report discusses an investigation into electro-optic directional couplers that use variable coupling in polymer-based waveguide structures. The approach begins with determining the desired response function, in this case a trapezoid. The Fourier transform method is then applied to synthesize the variable coupling function which results in the desired output response. This initial coupling function is iteratively modified using Newton's method to obtain a coupling design that can be implemented in a polymer waveguide. Approaches to achieving the variable coupling, including regions of negative coupling, are discussed.

14. SUBJECT TERMS

Electro-Optic Modulator, Optical Polymer Modulators, Directional Coupler, Polymer Optical Waveguide, Mach-Zehnder, Linearization Techniques, Spur Free Dynamic Range

15. NUMBER OF PAGES 26

16. PRICE CODE

17. SECURITY CLASSIFICATION OF REPORT	18. SECURITY CLASSIFICATION OF THIS PAGE	19. SECURITY CLASSIFICATION OF ABSTRACT	20. LIMITATION OF ABSTRACT
UNCLASSIFIED	UNCLASSIFIED	UNCLASSIFIED	UL

Table of Contents

1. Objective 1

2. Introduction 1

3. Design Technique for Coupler Modulators 1

4. Calculation of Switching Voltage-Length Products for different modulator designs 5

5. Distortion Calculations 12

6. Linearized Coupler Designs in Polymer Waveguides 14

6.1 Realization of Variable Coupling Designs in Polymer Waveguides 15

6.1.1 Variable Coupling Schemes 15

6.1.2 Negative Coupling by Phase Shifts 17

6.1.3 Electrode Structure for Polymer Coupler 17

7. Conclusions 18

8. References 19

List of Figures

1. Schematic of the uniform coupling coupler modulator. 2
2. The desired trapezoidal response function obtained after several iterations, the normalized intensity response plotted against the normalized switching voltage. 4
3. The iterated coupling function for the response function in figure 2. 4
4. Plot of normalized power against normalized distance along the coupler for different bias values. The power in the second guide of the coupler with trapezoidal response shown in figure 2. The blue curve is for zero bias, green is bias which obtains half power, and the red curve is bias when no transfer takes place into the second guide. 5
5. Schematic diagram of the Mach Zehnder modulator. 6
6. The Mach Zehnder calculated response. 7
7. Schematic diagram of the uniform coupler. 7
8. The response of the uniform coupler in which the normalized transmitted power is plotted against the normalized voltage. The value of p for this coupler is $\sqrt{3}/2$ for the push-pull case. 8
9. The linear response coupler modulator coupling function obtained from the Fourier transform of the desired linear response. 8
10. The linear response coupler modulator showing the response function as obtained from the coupling function in figure 9. 9
11. The trapezoidal response coupler design showing the coupling function. 9
12. The trapezoidal response coupler design showing the response function, desired and calculated. 9
13. The trapezoidal response coupler design from figure 11 showing the modified coupling function to have flat top regions. 10
14. The trapezoidal response coupler design from figure 13 showing the resultant response function. 10
15. The constant $|\kappa|$ coupler modulator design but with sign changes for the coupling. 11
16. The constant $|\kappa|$ coupler modulator but with sign changes for the coupling. The response function is shown, the value of p is 1.8 and the L/L_c ratio is 2.0. 11
17. The response function of the constant $|\kappa|$ coupler modulator design but with sign changes for δ along the length of the coupler. 12
18. The response function of the constant $|\kappa|$ coupler modulator but with sign changes for δ along the length of the coupler, the value of p is 2.7 and L/L_c is 3.0. 12
19. The trapezoidal response curve from figure 13 with the steep fall off region enlarged with the bias point at which the calculation was performed. 13
20. The distortion calculations showing the harmonics for a single tone at 10 GHz bias at midpoint in figure 19. 13
21. The distortion calculations showing the fundamental and the third harmonic generated intermodulation distortion (IMD3), with the different values marked by the bias points in figure 19. 14
22. The structure of the polymer waveguide for the Mach-Zehnder modulator, with the electrode structure modified to obtain 50 Ω impedance, velocity matched, and with 10 μm electrode thickness. 14
23. The variable coupling may be implemented by variable spacing, or by a third guide between the two guides of the coupler, or alternatively by varying the etching between the guides. 15
24. The variable coupling may be implemented by variable spacing between the guides, and for the basic coupler in the polymer guides with a spacing of 10 μm, and the range of coupling is also shown. 16
25. The variable coupling may be implemented by a third guide between the guides of the basic polymer coupler with a spacing of 10 μm, and the range of coupling is also shown. 16

26. The variable coupling may be implemented by varying the etching depth between the guides of the basic polymer guide coupler with a spacing of 10 μm, the range of coupling is shown. 16
27. The electrode structure with the even microstrip mode for the polymer coupler with its characteristic impedances shown. 17
28. The electrode structure with slow wave implementation for the coupler in even mode. 18
29. Microwave index for electrode structure in figure 28, even mode excitation. 18

List of Tables

I	Parameters for different materials for switching voltage length calculation.	5
II	Voltage-length product values for different designs, with p values and l/Lc for coupler designs.	6

1. Objective

The objective of this study was the linearization of optical modulator response in the variable coupling directional coupler modulator with particular emphasis on the realization in polymer waveguide structures.

2. Introduction

The co-directional coupler electro-optic modulator has an additional degree of freedom that is not available with the traditional Mach-Zehnder interferometric modulator. This additional parameter for the coupler modulator is the coupling function which can vary over the length of the device, and the variable coupling form may be synthesized to obtain the required response function. Thus, a linear response modulator may have its coupling function synthesized, and in fact a device of this type has been realized in GaAs/AlGaAs [1] previously. The synthesis method in this project uses the inverse Fourier transform method as a first guess, as it is can be shown that the coupling function and the output guide signal field are approximate Fourier transform pairs [2]. The synthesis then is performed using a modified form of Newton's method with this first guess as its initial value [3]. In this project the technique has obtained two linear modulator designs, and the switching voltages of these are compared to the traditional Mach-Zehnder and the uniform directional coupler designs.

The coupling functions synthesized by this technique have real values obtained by choosing symmetric response functions. However, these functions also have negative coupling regions, and the negative coupling regions are obtained by placing a π phase shift in one of the guides relative to the other. Subsequent return to positive coupling is obtained by inserting another phase shift region. In the linear modulator [2] this was realized by increasing the length of the one of the guides relative to the other. In the case of the GaAs/AlGaAs structure the effective index is about 3.4 at 1300 nm wavelength, and the required increase is 0.19 μm in one of the guides. In the case of the polymer guide with an effective index of 1.61, this increase in length is about 0.4 μm. However, for polymer guides, which are low contrast structures, the bend radii for insertion of this extra length is large, of the order of millimeters for low loss and in these structures a different approach was required. The technique suggested is a section of the coupler in which the two guides have slightly different effective indices, and by choosing an appropriate length the phase shift of π may be readily obtained.

The electrode structure of the current polymer guide Mach-Zehnder modulators are microstrip lines with the Au metallization of about 1 μm thickness, and 8 μm wide. The skin depth in Au metallization at 1 GHz is about 3 μm, which leads to a lossy electrode structure. In this report a low loss Au metallization design for the existing Mach-Zehnder modulators has been obtained. For the coupler modulator, the microstrip lines on the two guides become coupled and thus even and odd modes may be obtained by the form of excitation. In this case, it is suggested that the even mode be used, with the polymer poled in opposite directions under the two electrodes to provide the necessary push pull effect. However, in this case the impedance of the even mode microstrip line is of the order of 35 ohms, including the slow wave structure for matching the phase velocity and the optical guide velocity. For even mode excitation, the domains under the two optical waveguides would have to be reverse poled. Using the odd mode excitation for this line results in higher impedance, but this was not examined due to time constraints.

The following sections summarize the work in these areas.

3. Design Technique for Coupler Modulators

The schematic diagram for the coupler is shown in Figure 1, with the two guides in close proximity to each other, with the input to guide one given as *R(0)* and the input to the second guide *S(0)*. When a signal is placed on the first guide of the uniform coupler modulator, both the even and odd supermodes of this

coupler are excited, with the modes adding constructively in this first guide and destructively in the second guide. The signal which is now the superposition of the two modes travels down the coupler with the odd mode velocity being slightly higher. A specific distance later the phases of the odd and even modes are interchanged because of the difference in velocities, so that the modes add constructively in the second guide, but destructively in the first, in effect causing a transfer of power from guide one to guide two.

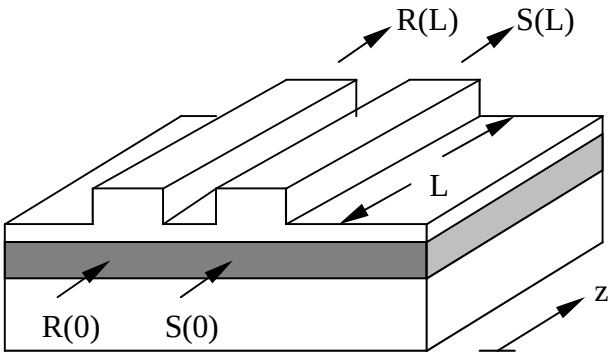

Figure 1: Schematic of the uniform coupling coupler modulator

The coupled mode equations for the directional coupler are given by:

$$\frac{\partial R}{\partial z} = j\delta R - j\kappa(z) S e^{-j\phi(z)}$$
$$\frac{\partial S}{\partial z} = -j\delta S - j\kappa(z) \mathrm{Re}^{j\phi(z)} \tag{1}$$

where R and S are the complex amplitude fields in the guides as a function of z, spatial position along the coupler, κ(z) is the coupling coefficient which is a slowly varying function of z, Δβ is the difference in the propagation constants of the two guides uncoupled, δ = Δβ/2, and

$$\phi(z) = \int_0^z [\Delta\beta(z') - \Delta\beta(0)] dz' \tag{2}$$

In the directional coupler modulator, the guides are made identical to each other, so that δ is zero in the unbiased condition, and the application of bias makes Δβ nonzero, and hence δ is also nonzero.

The solution to these equations for a uniform coupler of length L, with initial conditions of *R(0)* =1 and *S(0)* =0, is given by:

$$R(L) = \cos\left(L\kappa\sqrt{1+(\delta/\kappa)^2}\right) + \frac{j\delta \sin\left(L\kappa\sqrt{1+(\delta/\kappa)^2}\right)}{\sqrt{1+(\delta/\kappa)^2}} \tag{3}$$

$$S(L) = \frac{-j \sin\left(L\kappa\sqrt{1+(\delta/\kappa)^2}\right)}{\sqrt{1+(\delta/\kappa)^2}} \tag{4}$$

The amplitude response of the uniform coupler modulator is given by:

$$\eta \equiv |S(L)|^2_{R(0)=1,S(0)=0} = \frac{-j\sin^2(L\kappa\sqrt{1+(\delta/\kappa)^2}}{1+(\delta/\kappa)^2} \tag{5}$$

Define the coupling length L_c as the distance where all the power in the first guide of the uniform coupler is transferred to the second, or |S| = 1. In the case when there is no bias which implies $\delta = 0$, then from the above equation $L = L_c = \pi/(2\kappa)$. For the case when bias is applied so that δ is not zero, then for $L = L_c$, for $S = 0$, $\delta_{switch}/\kappa = \sqrt{3}$ or $\delta_{switch} L_c = \sqrt{3}\pi/2$. Also when the two guides are biased so as to have different effective indices, then by definition

$$\delta = \Delta\beta/2 = (n_{guide1} - n_{guide2})\pi/\lambda_0 = 2\Delta n_{guide}\pi/\lambda_0 \tag{6}$$

The difference in the guide effective indices due to bias is given by [2]

$$\Delta n_{guide} = (n^3 r_{xx} V\Gamma)/2d \tag{7}$$

where n is the guide mean effective index, r_{xx} is the electro-optic coefficient depending on the direction of the field interacting with the optical mode, V is the voltage applied to the coupler electrodes, d is the distance between the electrodes, and Γ is the overlap integral between the bias electric field and the electric field of the optical mode. Substituting for the δ from the above equation :

$$V_{switch} L_c = p(\lambda_0 d)/(n^3 r\Gamma) \tag{8}$$

where

$$p = \delta_{switch} L_c/\pi = \sqrt{3}/2 \tag{9}$$

for push pull electrode excitation of the uniform coupler.

Using the transformation to the Ricatti equation [1,2], it can be shown for very small coupling that S and κ are related through the Fourier transform equation of the form:

$$\kappa(z) = \frac{2}{\pi}\int_0^\infty |S(\delta)|\cos(2\delta z)d\delta \tag{10}$$

Thus, if the desired intensity response for the coupler modulator is given by $|S(\delta)|^2$, the first guess with small coupling is obtained from the above equation (10). The coupling function derived from this equation extends to $\pm\infty$, and needs to be truncated symmetrically to prevent chirp being generated. The truncated coupling function will only provide an approximate form of the desired response, and thus needs to be modified to provide a closer agreement. The next step uses the Newton's method [3], with this truncated response as the first guess. The error in the response function is evaluated, the appropriate Jacobian is obtained, and by the least squares method the correction is obtained. Subsequent iterations move the coupling function closer to the desired response function. Figure 2 shows the desired response function in the form of a trapezoid and the iterated response from the modified coupling function is shown in Figure 3.

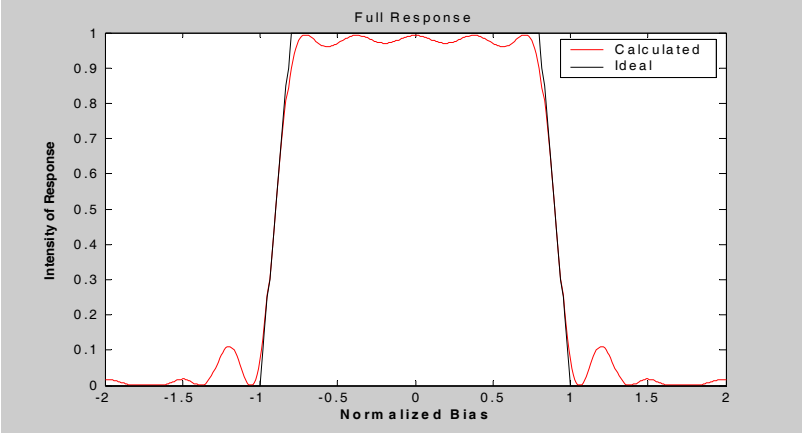

Figure 2: The desired trapezoidal response function obtained after several iterations, the normalized intensity response plotted against the normalized switching voltage.

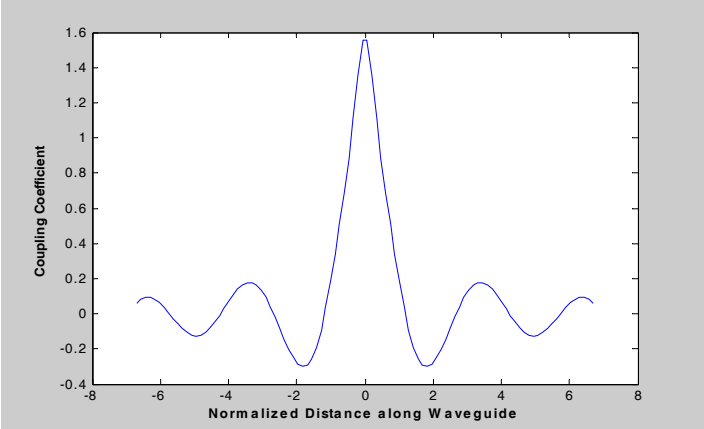

Figure 3: The iterated coupling function for the response function in figure 2.

The power in the second guide along the coupler is shown in Figure 4. Note that, for the zero bias case, shown in blue, the transfer of power to the second guide only takes place in the major lobe of the coupling function in the center of the coupler. Thus, the regions of small coupling at the ends of the coupling function contribute to shaping the response function. The green curve shows the power in the guide with bias halfway down the trapezoidal slope region. It becomes apparent that the power is initially transferred to the second guide, and then half of it returns to the first guide to obtain a final value of half. The red curve shows the modulator biased to zero output at the second guide, with initial transfer, and then the power returning entirely to the first guide.

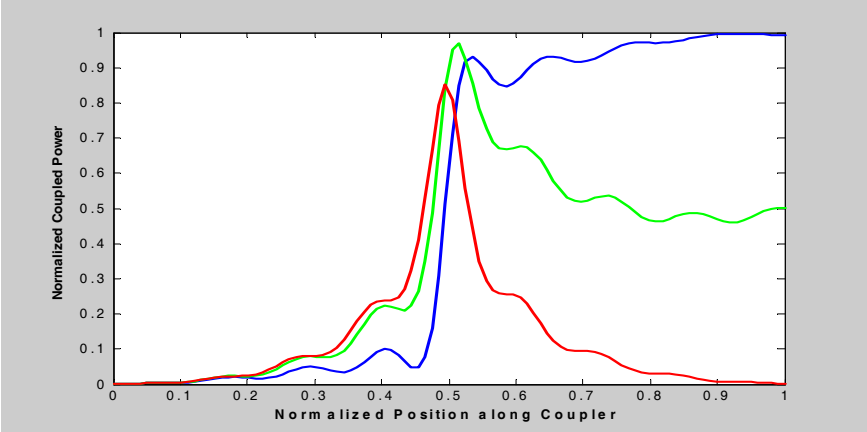

Figure 4: Plot of normalized power against normalized distance along the coupler for different bias values. The blue curve is for zero bias, green curve is for bias which obtains half power, and the red curve is for bias when no transfer takes place into the second guide.

4. Calculation of Switching Voltage-Length Product for Different Modulator Designs

When the guide electrodes of a modulator are biased, the index in the guides vary resulting in $\Delta\beta$ becoming non-zero, and in turn this results in δ becoming nonzero. As shown above for the push pull bias, the product of the switching voltage V_{switch} and the modulator length L_c is given by the equation:

$$V_{switch}L_c = p\frac{\lambda_0 d}{n^3 r_{xx}\Gamma} \tag{11}$$

where p is given by $\delta_{switch}L/\pi$, and is the figure of merit for the designs, Γ is the overlap integral between the optical field and the bias field, d is the electrode gap, n is the effective index, r_{xx} is the electro-optic coefficient for the geometry being used. For the Mach-Zehnder interferometric modulator p is 0.5, and for the constant coupling coupler modulator p is 0.87. Table I provides the electro-optic constants for different materials used for the switching voltage-length calculations, together with other parameters.

Table I: Parameters for different materials for the switching voltage-length calculation.

Parameters	**CLD-75 Polymer**	**GaAs/$Al_{0.2}Ga_{0.8}As$**	**$LiNiBO_3$**
Wavelength (nm)	1550 nm	1550 nm	1550 nm
Electrode Spacing d (μm)	8 μm	2 μm	8 μm
Overlap integral Γ	0.95	0.65	0.55
Electro-optic coefficient r_{xx}	36 pm/V	1.43 pm/V	31.5 pm/V
Refractive index n at 1550 nm	1.612	3.43	2.138
$n^3 r_{xx}$	150	58	308
Ratio $(V_{switch} L)/ p$	8.66 V-cm	8.26 V-cm	7.32 V-cm

Table II: Voltage–length product values for different designs, with p values, and L/L_c for coupler designs.

Modulator Design	**p**	**L/L_c**	**CLD-75 Polymer**	**$GaAs/Al_{0.2}Ga_{0.8}As$**	**$LiNiBO_3$**
Uniform coupler	0.87	1	7.5 V-cm	7.15 V-cm	6.3 V-cm
Mach-Zehnder	0.5		4.33 V-cm	4.13 V-cm	3.66 V-cm
Coupler: Trapezoidal response	1.2	1	10.4 V-cm	9.9 V-cm	8.8 V-cm
Coupler: Linear response	4.1	1	35.5 V-cm	33.9 V-cm	30.0 V-cm
Coupler: constant κ, π phase shifts	1.8	2	15.6 V-cm	14.9 V-cm	13.2 V-cm
Coupler: δ varied, constant κ	2.7	3	23.4 V-cm	22.3 V-cm	19.8 V-cm

The spacing for the $GaAs/Al_{0.2}Ga_{0.8}As$ modulator with Schottky contacts has all the voltage drop in the depletion layer. Although the electrode spacing may be 8 μm to be consistent with the other cases, a realistic value here depends on the intrinsic unintentional doping level. This was chosen to be 2 μm on average for both MBE and MOCVD material. Note that the semiconductor estimate is at best approximate since the depletion layer thickness varies as the square root of the sum of the bias voltage and the Schottky barrier built-in voltage.

Congruent $LiNiBO_3$, as opposed to the stoichiometric $LiNiBO_3$, is widely used and its value of r_{31} was used in the above Table I. The overlap integral Γ has been widely quoted as 0.20 for lithium niobate, and our earlier estimate of the ratio $(V_{switch}\, L)/\, p$ in this material obtained a value of 17.9 V-cm with this value of Γ. However, recent discussions with Dr. SriRam of Srico Inc. has provided us with a better estimate of 0.55 for the z-cut structures and this has resulted in the ratio $(V_{switch}\, L)/\, p$ shown in Table I.

The various designs that have been examined in this study are listed in Table II together with their $V_{switch}\, L$ values in the appropriate material system. In the following figures the different designs are shown with the corresponding intensity versus bias voltage response curves. Figures 5 and 6 show the schematic diagram of the Mach-Zehnder interferometric modulator and its calculated response function with a straight line linear response showing the deviation respectively. The calculated value of p is 0.5 for the push pull case.

Figure 7 shows the schematic diagram of the uniform coupler, and Figure 8 shows the response function, the value of p for this device is 0.866 $(=\sqrt{3}/2)$. The linear response coupler case obtained the coupling from the Fourier transform, as shown in Figure 9, and the corresponding response in Figure 10 for the truncated coupling function.

The trapezoidal response coupler design coupling function is shown in Figure 11 and the response function in Figure 12, desired and calculated. Since the realization of this coupling function is difficult, the alternative coupling function with flat topped regions and the corresponding response function, which has suffered from this modification, are shown in Figures 13 and 14.

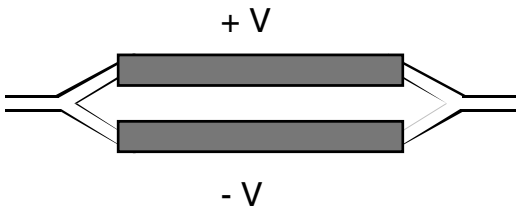

Figure 5: Schematic diagram of the Mach Zehnder modulator

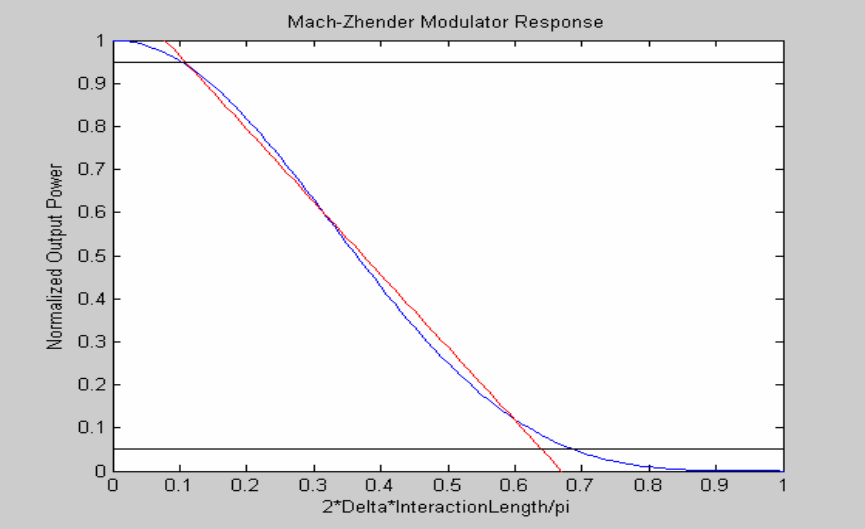

Figure 6: The Mach Zehnder calculated response.

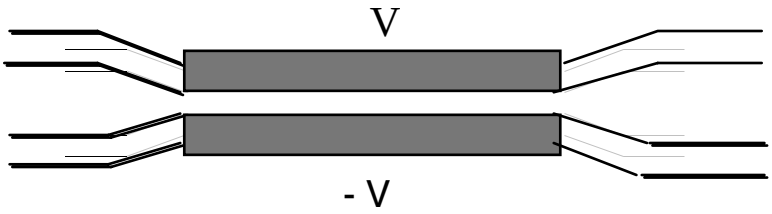

Figure 7: Schematic diagram of the uniform coupler.

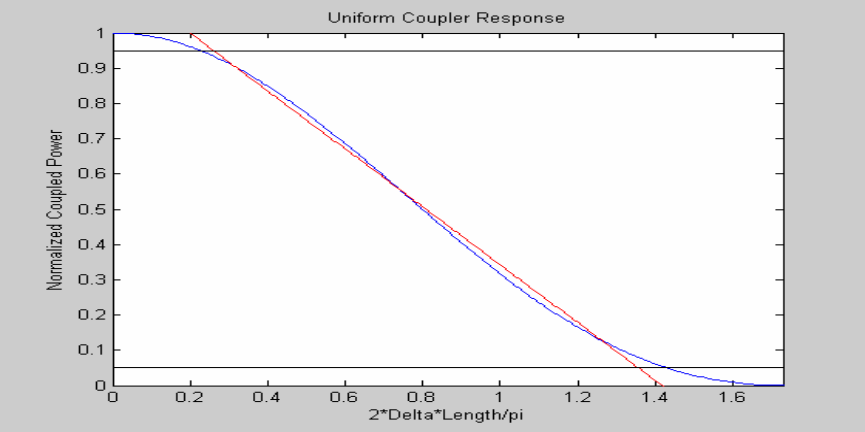

Figure 8: The response of the uniform coupler in which the normalized transmitted power is plotted against the normalized voltage. The value of p for this coupler is $\sqrt{3}/2$ for the push pull case.

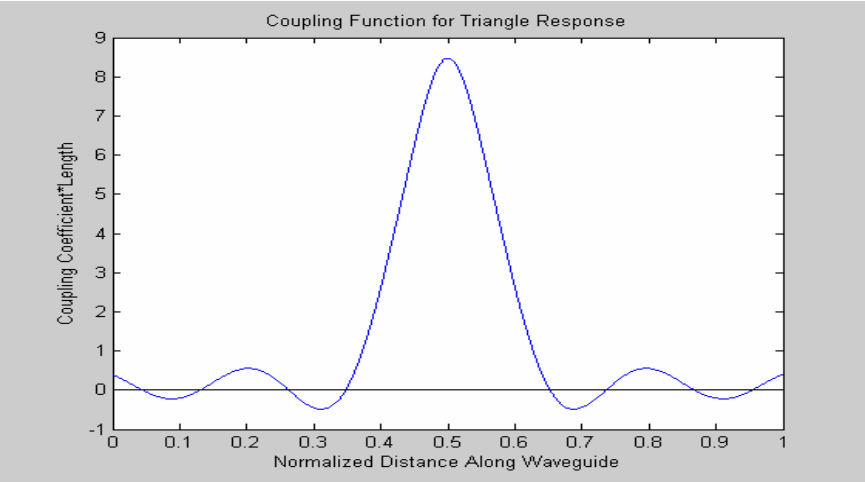

Figure 9: The linear response coupler modulator coupling function obtained from the Fourier transform of the desired linear response.

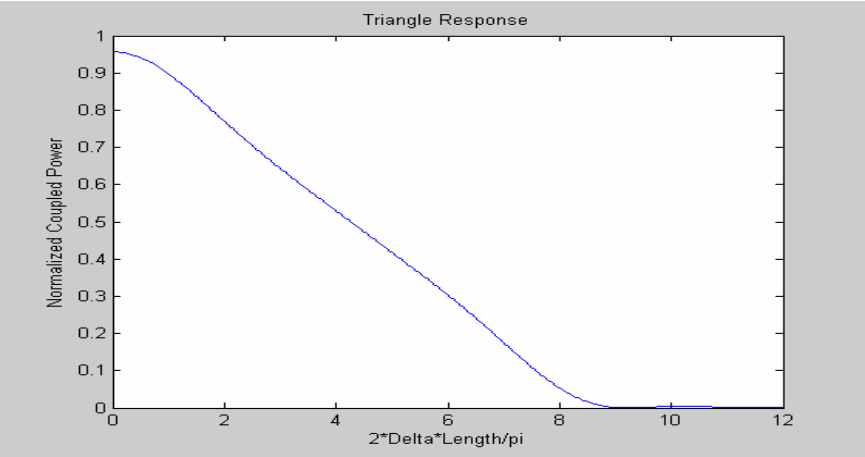

Figure 10: The linear response coupler modulator showing the response function as obtained from the coupling function in figure 9.

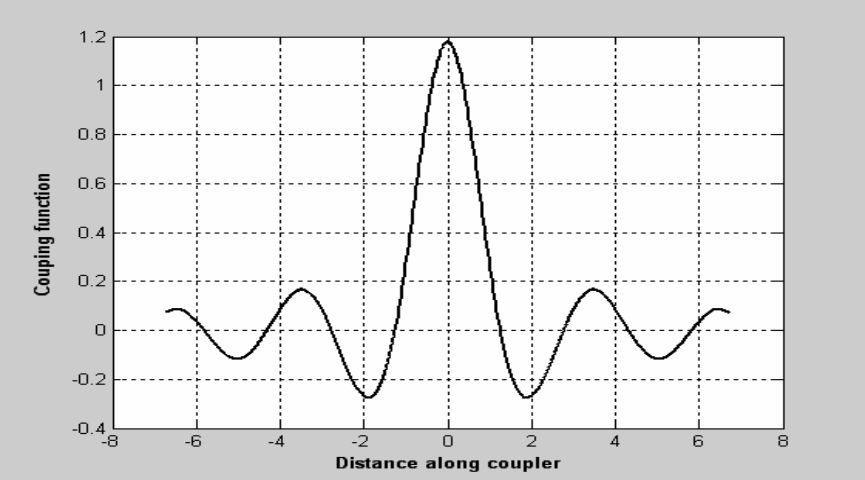

Figure 11: The trapezoidal response coupler design showing the coupling function.

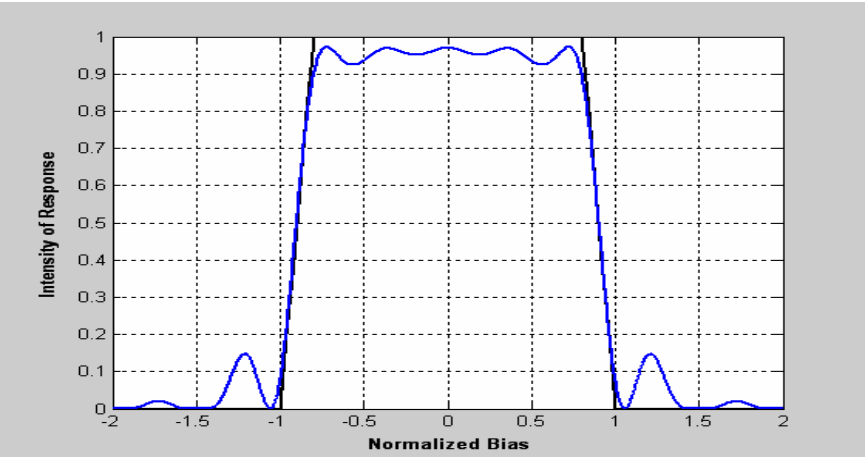

Figure 12: The trapezoidal response coupler design showing the response function, desired and calculated.

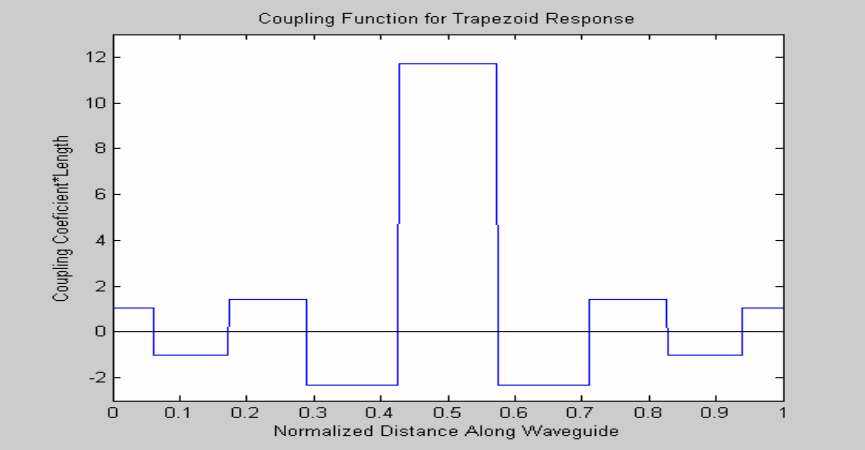

Figure 13: The trapezoidal response coupler design from figure 11 showing the modified coupling function to have flat top regions.

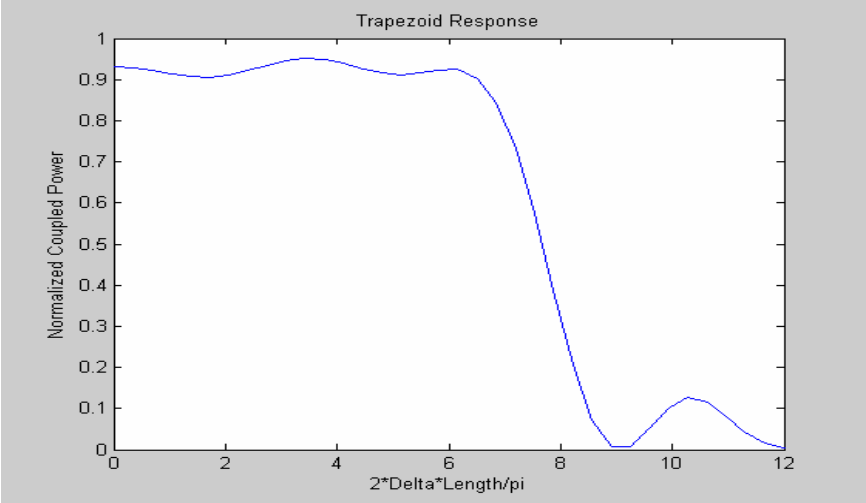

Figure 14: The trapezoidal response coupler design from figure 13 showing the resultant response function.

Two other designs are also considered. In the first design, the coupling is made positive or negative but retains a constant magnitude. This is to be achieved by placing 180 degree phase shifts at the sign change positions, and this is discussed further in the following section. The second design maintains κ constant but switches the sign of δ in the biased condition, either by having segmented electrodes which are biased alternately with opposite polarities or by poling the material, polymer or $LiNiBO_3$ or other ferroelectric material in alternate directions. In the former, the effect of the sign change for κ results in a slight dip in the transfer of power along the coupler, but ultimately results in a very linear response function as shown in Figure 15 and Figure 16 for a longer device of twice the coupling length, with p=1.8. In the latter case, the change in bias is similar to the delta-beta coupler modulators, but also allows the use of poling to obtain this voltage bias change with continuous electrodes. In this case adjusting the positions and the lengths of the poled sections results in a linear response modulator as shown in Figures 17 and 18 with the device length three times the coupling length, and p having a value of 2.7.

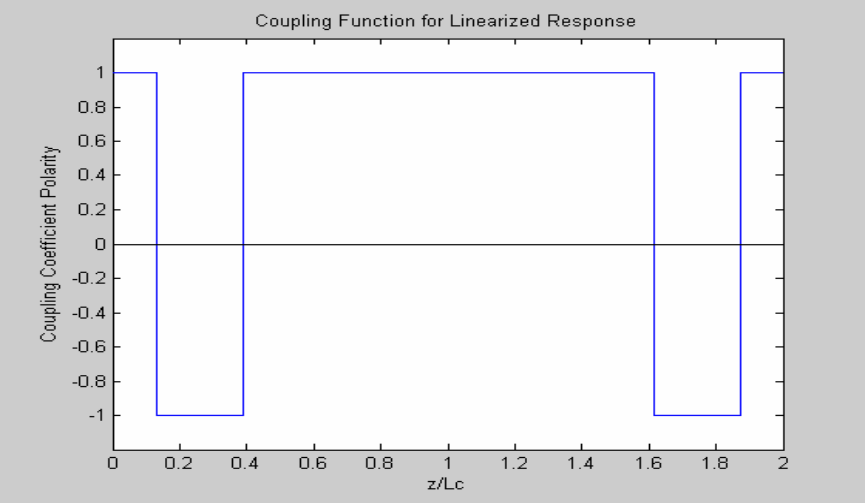

Figure 15: The constant |κ| coupler modulator design but with sign changes for the coupling.

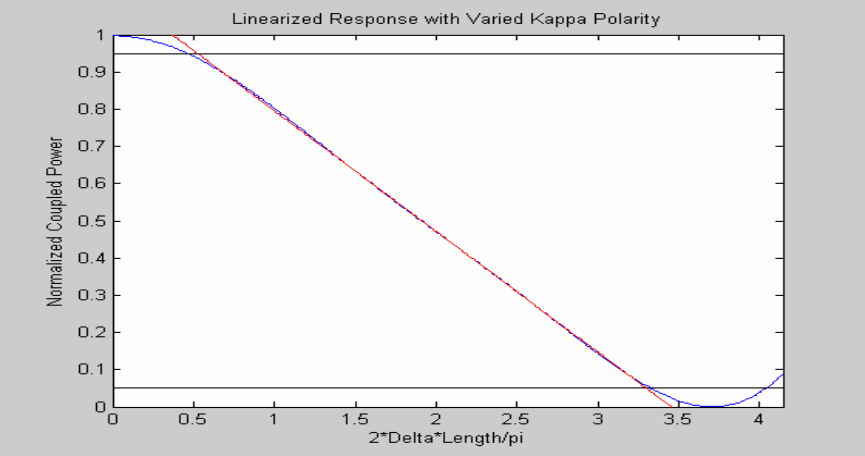

Figure 16: The constant |κ| coupler modulator but with sign changes for the coupling. The response function is shown, the value of p is 1.8 and the L/L_c ratio is 2.0.

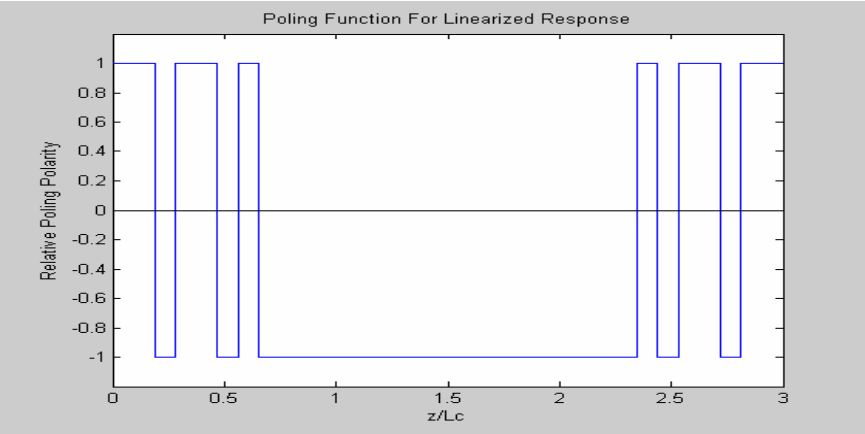

Figure 17: The constant |κ| coupler modulator design but with sign changes for δ along the length of the coupler.

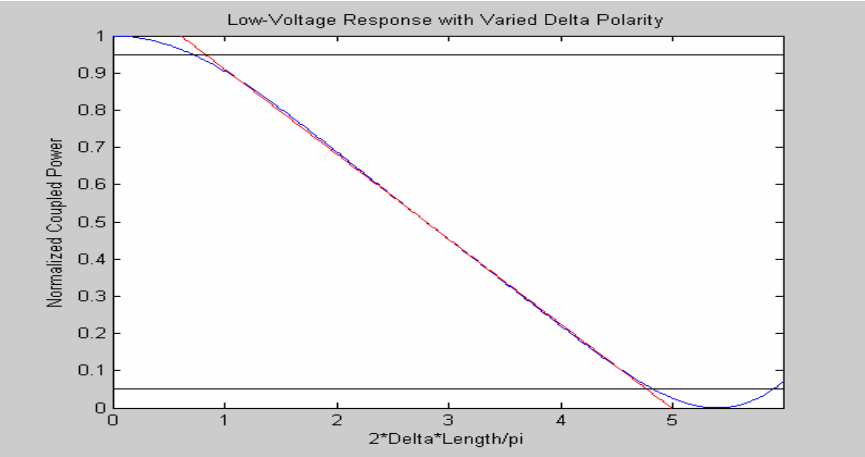

Figure 18: The response function of the constant |κ| coupler modulator but with sign changes for δ along the length of the coupler, the value of p is 2.7 and L/L_c is 3.0.

5. Distortion Calculations

The usual technique for calculating the distortions in modulators is to express the response function as a polynomial in the applied voltage, and thus for the present case the output signal power is expressed as:

$$|S|^2_{out} = a_0 + a_1 V_{appl} + a_2 V^2_{appl} + a_3 V^3_{appl} + ...$$

(12)

However, expressing the response function in polynomial form results in considerable error and the results are not accurate.

Another method is to superpose two signals at slightly different frequencies, sum them and take the Fourier transform, either in the FFT technique or in the usual integral form. However, it is necessary that periodicity is not violated by taking too small a sequence, and this is also results in inaccuracies due to the large number of points required. The most accurate method is to use the 2D FFT technique in which the two dimensions correspond to the time periods of the two tones passed through the modulator simultaneously. Matlab and other programs have this as a standard function, but it is also possible to program it to work with the single FFT code. Figure 19 shows the trapezoidal response function, with the enlarged section of the response curve. Figures 20 and 21 show the harmonics and the intermodulation distortion third harmonic (IMD3), which are $2f_1 - f_2$ and $2f_2 - f_1$ components with different drive levels. Drawing the noise floor provides the spur free dynamic range (SFDR), which is the vertical distance from the intersection of the noise floor of the IMD3 line to the fundamental power at that point.

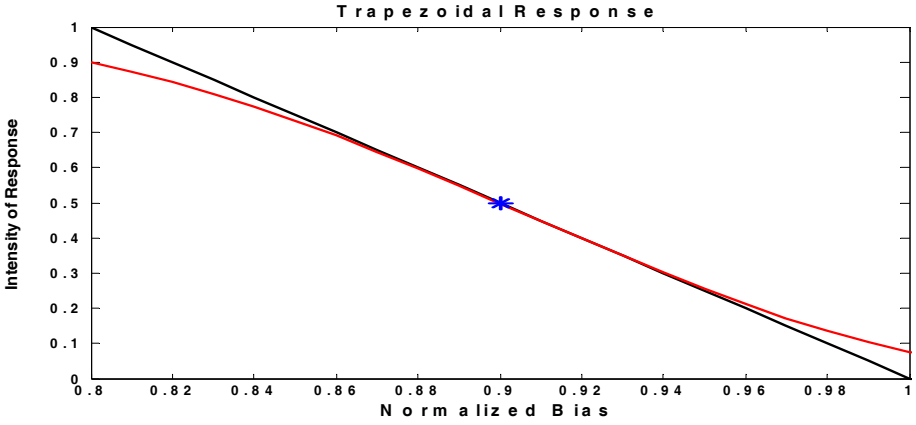

Figure 19: The trapezoidal response curve from figure 13 with the steep fall off region enlarged with the bias point at which the calculation was performed.

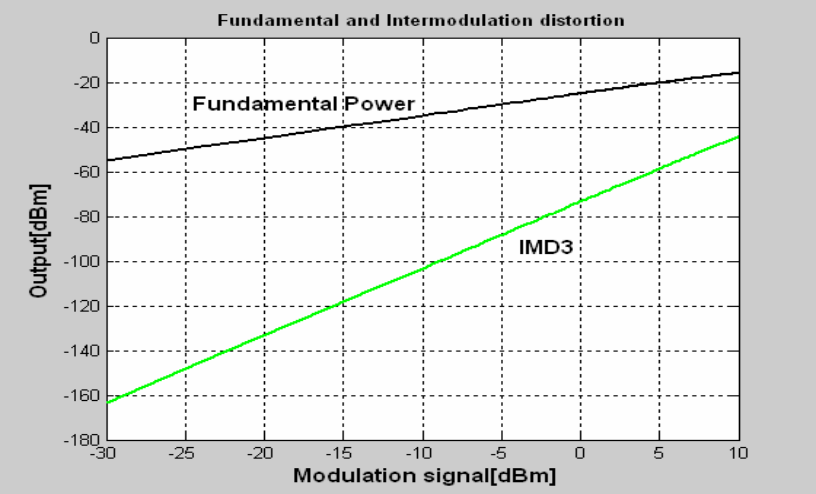

Figure 20: The distortion calculations showing the harmonics for a single tone at 10 GHz bias at midpoint in figure 19.

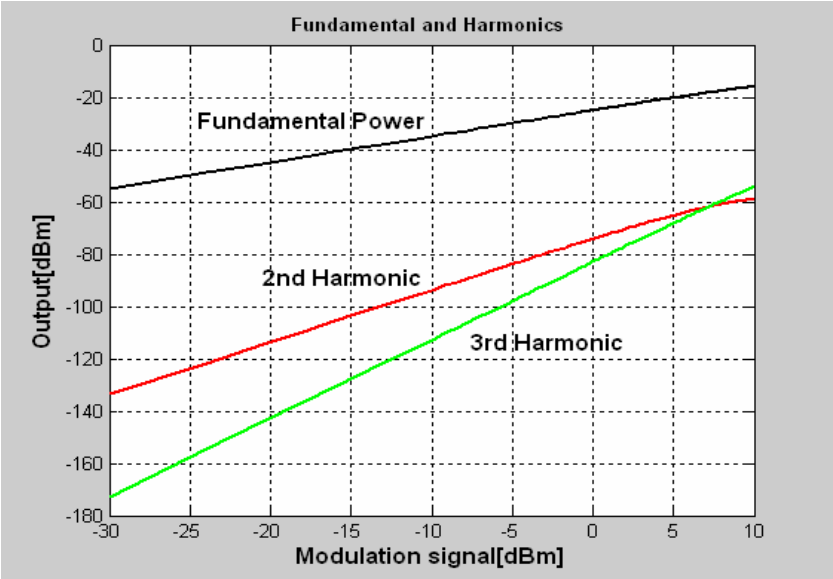

Figure 21: The distortion calculations showing the fundamental and the third harmonic generated intermodulation distortion (IMD3), with the different values marked by the bias points in figure 19.

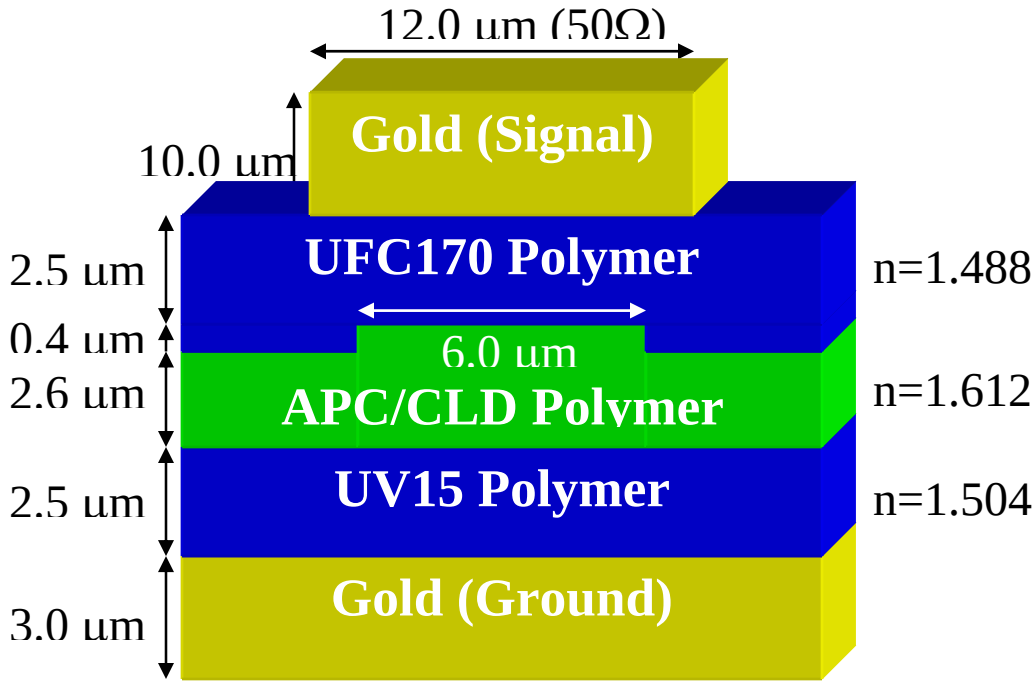

Figure 22: The structure of the polymer waveguide for the Mach-Zehnder modulator, with the electrode structure modified to obtain 50 Ω impedance, velocity matched, and with 10 μm electrode thickness.

6. Linearized Coupler Designs in Polymer Waveguides

The polymer modulator guide structure is shown in Figure 22 from the work of the USC-UCLA groups [4], except that the width of the electrode structure is 12 μm and the thickness is 10 μm, as per calculations performed in this project for velocity matched 50 Ω microstrip line. The original design for their Mach-

Zehnder modulator had 8 μm wide electrodes, 1 μm thick, leading to a velocity matched microstrip line with impedance of 70 Ω for the individual lines. The polymer guides are poled with bias on the electrodes in the Mach-Zehnder modulator, and in the coupler it is suggested that this type of poling is performed in which the two guides are in oppositely poled material. Since our design suggest a 10 μm spacing, it will be necessary to ensure that surface breakdown does not prevent poling to take place. If this cannot be performed successfully, then we will have to alter our electrode design from the coupled even mode slow wave structure to the odd mode slow wave structure.

6.1 Realization of Variable Coupling Designs in Polymer Waveguides

6.1.1 Variable Coupling Schemes

The variable coupling designs may be implemented using alternative approaches as shown in Figure23.

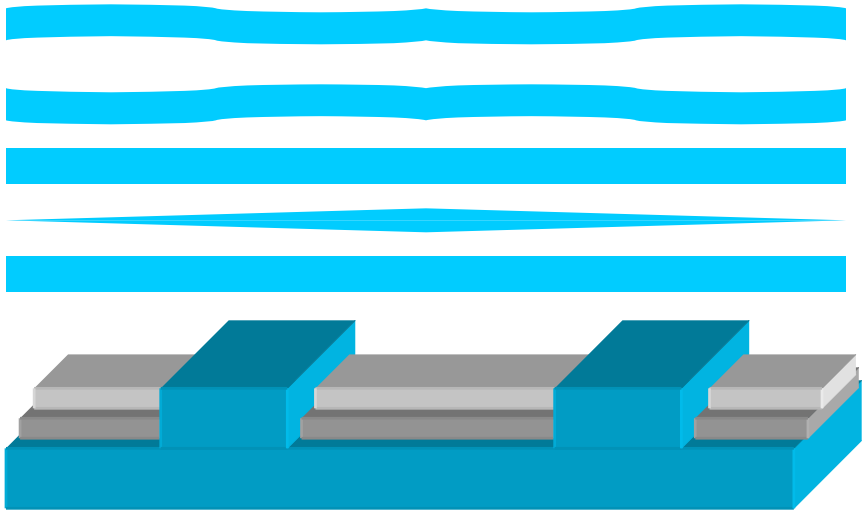

Figure 23: The variable coupling may be implemented by variable spacing, or by a third guide between the two guides of the coupler, or alternatively by varying the etching between the guides.

The simplest method is the variable spacing scheme, however, the problem of electrodes following the variable spacing remains, and since this changes the electrode impedance this needs to be accounted for. Beam propagation code from RSoft was used to determine the range of coupling that may be implemented with this method, and the results are shown in Figure 24. These results show that this is the simplest method of implementing the variable coupling concept, with a wide range of coupling that may be implemented, and a smoothly varying coupling function may also be implemented.

The second scheme is to place a third guide between the guides of the coupler. In this case, the third guide needs to be single mode to ensure that no multimode propagation occurs, and also it is necessary to retain the basic odd and even mode structure of the coupler, so that only this basic eigenvector of this three guide coupler is excited. The range of coupling that may be obtained with this method is limited to a two to one ratio as shown in Figure 25, obtained with the RSoft BeamProp program. The calculations show that a smoothly varying coupling function may also be implemented within this range of variation.

The third scheme is to have the gap between the coupled guides constant, but to vary the etch depth between them. While a wide range of coupling may be obtained with this method, the problem is that when the cladding surface approaches the guide layer, the mode becomes very lossy, due to the etch roughness. Figure 26 shows this for the polymer coupler, again using BeamProp for the calculations.

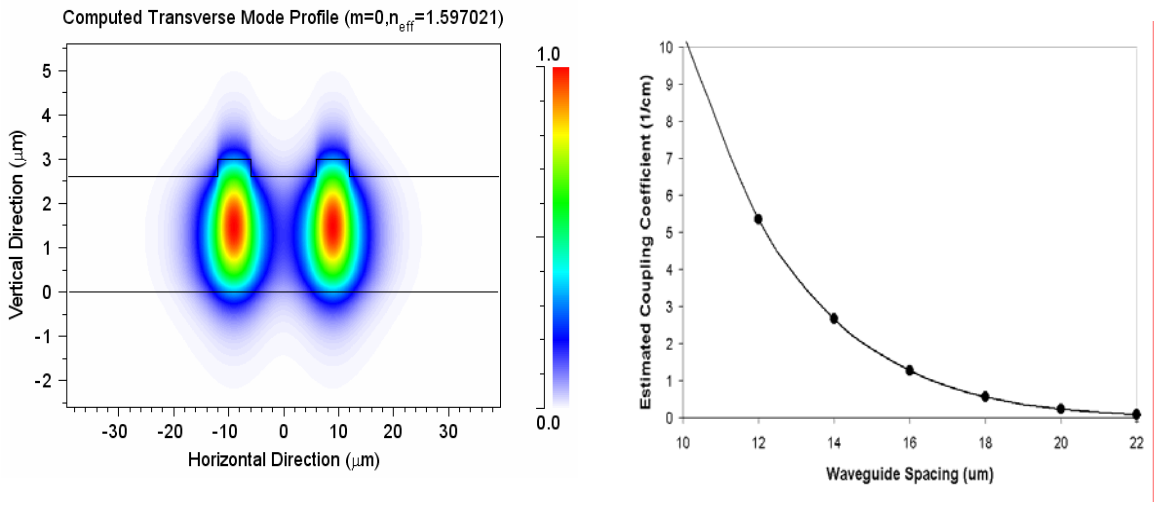

Figure 24: The variable coupling may be implemented by variable spacing between the guides, and for the basic coupler in the polymer guides with a spacing of 10 μm, and the range of coupling is also shown.

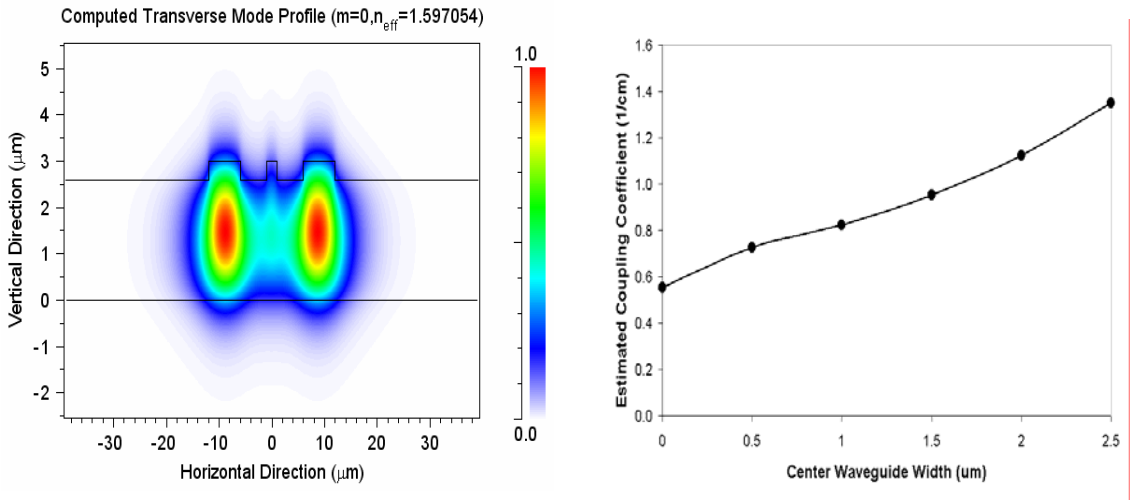

Figure 25: The variable coupling may be implemented by a third guide between the guides of the basic polymer coupler with a spacing of 10 μm, and the range of coupling is also shown.

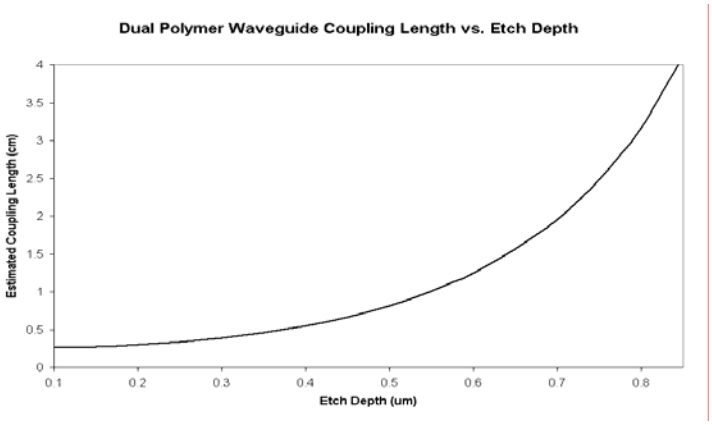

Figure 26: The variable coupling may be implemented by varying the etching depth between the guides of the basic polymer guide coupler with a spacing of 10 μm, the range of coupling is shown.

6.1.2 Negative Coupling by Phase Shifts

Negative coupling may be implemented by placing a relative phase shift between waveguides. This requires one waveguide to be $\lambda/2$ longer than the other. In semiconductor waveguides, in our previous work [3], the gap was increased between the guides and then an increased $\lambda/2$ length was added to one of the guides, in the form of a section of a loop, and the loop radii were in the region of 100 μm or larger. In polymer guides, this requires bends with 0.48 mm or larger radii, which makes these rather long. The alternative is to use a polymer coupler with different waveguide refractive indices to produce this phase shift. Thus, leaving one guide unpoled produces 180degrees phase shift in 40 μm. Implementation of this is thus very simple and does not require the loop phase shifter.

6.1.3 Electrode Structure for Polymer Coupler

The skin effect thickness of gold electrodes, traditionally used in modulators at 1 GHz is about 3 μm and therefore it is necessary to have electrodes with thickness of 10 μm to have minimum conductor loss for modulation at 10 GHz upwards. The polymer guides use microstrip lines for their electrodes and the widths are adjusted so that the phase velocity is close to the velocity of light in the guides, c/1.6. In the case of the polymer coupler, coupled microstrip lines are used in the even mode, so that the optical guide regions under the two guides are poled in opposite directions. With 10 μm thick electrodes considerable energy propagates in the air, and so these become fast wave structures, and to velocity match them we need to introduce additional electrodes which form slow wave structures. However, the impedance suffers, as this is now in the 35 Ω range. These are shown in Figures 27, 28 and 29.

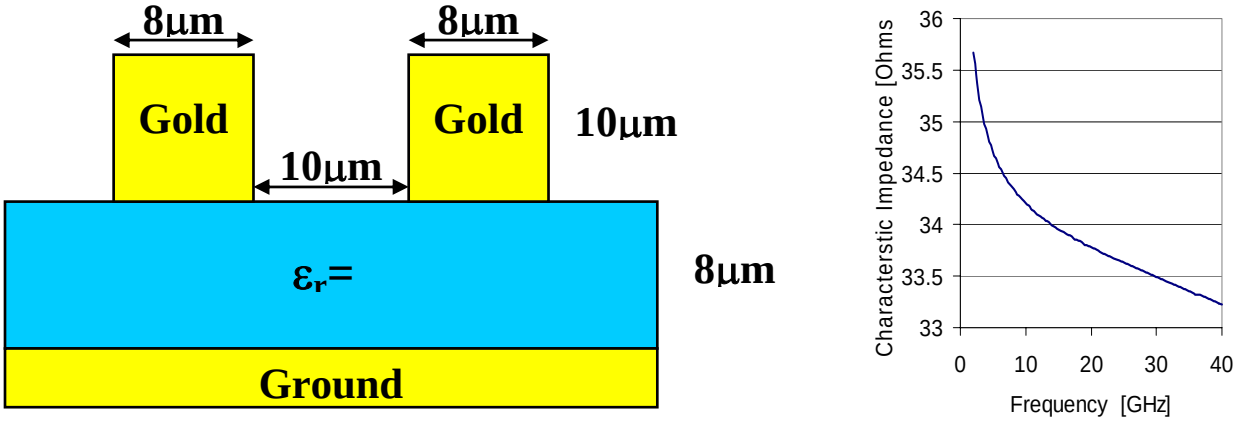

Figure 27: The electrode structure with the even microstrip mode for the polymer coupler with its characteristic impedances shown.

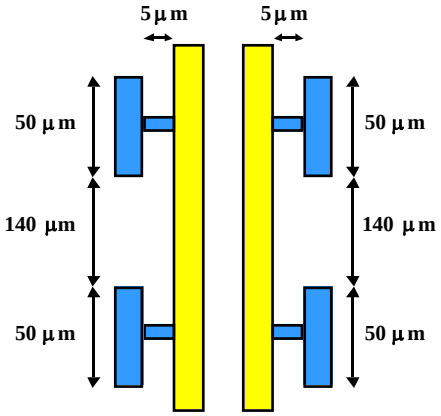

Figure 28: The electrode structure with slow wave implementation for the coupler in even mode.

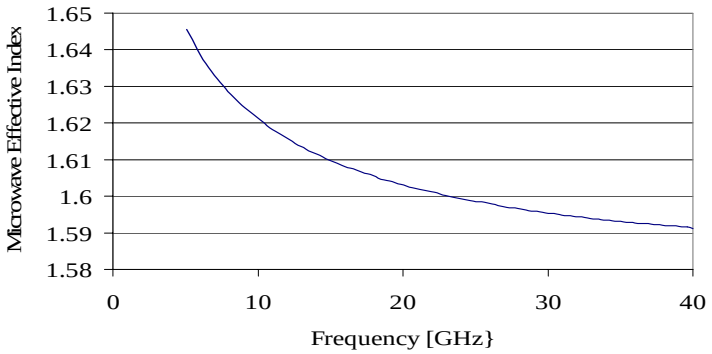

Figure 29: Microwave index for electrode structure in figure 28, even mode excitation.

7. Conclusions

The project conducted a study of two aspects of the variable-coupling linear response directional coupler modulator. The first part of the study determined the optimum method of synthesizing the coupling function for linear response in conjunction with the implementation constraints. The second part of the study examined the problems involved in implementing the variable-coupling linear response directional coupler modulator in polymer waveguides. In conclusion, this study shows that variable coupling directional coupler modulators with ultra-linear response may be readily realized in polymer waveguides.

8. References

1. C. Laliew, S. Lovseth, X. Zhang, A. Gopinath: Linear optical coupler modulators, J. Lightwave Tech., Vol. 18, pp. 1244 -1249, 2000.
2. T. Tamir, Editor, *Guided Wave Optoelectronics*, Springer-Verlag, second edition, 1988
3. T. Li, C. Laliew, A. Gopinath, An iterative transfer matrix inverse scattering technique for synthesis of co-directional couplers and filters, J. Quantum Electronics, vol. 38, pp.375-379, April 2002.
4. M.-C. Oh, H. Zhang, C. Zhang, H. Erlig, Y. Chang, B. Tsap, A. Szep, W. H. Steier, H. R. Fetterman, L. R. Dalton, Recent advances in electrooptic polymer modulators incorporating highly nonlinear chromophores, IEEE J. Special Topics in Quantum Electronics, vol. 7, pp. 826-35, 2001.